JMEPEG (1992) 1:323-332

Modeling and Analysis of Journal Bearings Lubricated with Molten Zinc for Galvanizing Process

M. Rashidi

The production speed of the steel sheet galvanizing process is limited by several factors; the dynamic behavior of the guiding rollers submerged in a molten zinc bath is among the crucial ones. These guiding rollers are supported on journal bearings operating on molten zinc, which acts as the lubricant of the bearings. This article addresses the modeling of journal bearings of this type as a two degrees of freedom system. The molten zinc film thickness is treated as a set of the classical hydrodynamic coefficients (stiffness and damping elements) to study the bearing dynamics and vibration stability, as well as the minimum film thickness formation. Computer-simulated test cases of the bearing geometry, zinc alloy viscosities at different temperatures, and operating conditions demonstrate the stable bearing performance at a desired galvanizing production speed.

1. Introduction

RECENT advents in software/hardware computational tools have changed the course of optimum manufacturing process developments from an experimental trial-and-error procedure to that of mathematical modeling and computer simulations. Unexplainable and not well-understood aspects of manufacturing processes used to be categorized as the "art of manufacturing." Tedious experimental trial-and-error methods, expensive by nature and confined in result yields, were considered the only effective means to solve a manufacturing problem.

The manufacturing of thin galvanized metal sheet has ample room for the use of mathematical modeling and computer simulation. Galvanized sheet production is measured by scales of millions of tons per year. However, some fundamental manufacturing problems are encountered and have not been addressed effectively. These problems are ignored at the expense of lower productivity and lower production speeds. For example, the galvanizing process of thin metal sheets is conducted at low speeds to ensure product quality.

Increases in productivity and quality assurance are obtained via a reasonable understanding of the dynamics of the machinery involved in the manufacturing of galvanized sheet. Dynamics and control of the metal sheet passing through a molten zinc bath and vibration characteristics of the guiding rollers submerged in the molten zinc bath are among the factors that limit the production speed of the galvanizing process. This article addresses the study and analysis of the journal bearings that support the guiding rollers of a galvanizing process.

2. Statement of the Problem

Figure 1 shows a schematic view of the typical equipment and stages of the galvanizing process. As illustrated in this figure, the metal sheet is passed through a furnace to elevate its temperature. Then, it is submerged into a bath of molten zinc, passing over two or three rollers, and eventually an air knife

M. Rashidi, Mechanical Engineering Department, Cleveland State University, Cleveland, Ohio.

Nomenclature

B = Index for backward mode of journal whirl
c = Radial clearance of journal bearing
C_{mn} = Dimensionless damping of lubricant film
$\overline{C}_{mn}$ = Dimensional damping of lubricant film
D = Bearing diameter
d = Derivative symbol
E_{cyc} = Energy imparted to journal during one cycle of its orbital motion
F = Index for forward mode of journal whirl
$f_x(t)$ = External force exerted on journal whirl in x direction
$f_y(t)$ = External force exerted on journal whirl in y direction
$_{m,n}$ = Index for x and y
$j = \sqrt{-1}$
K_{mn} = Dimensionless stiffness of lubricant film
$\overline{K}_{mn}$ = Dimensional stiffness of lubricant film
L = Bearing length
M = Dimensionless mass supported by a bearing
$\overline{M}$ = Dimensional mass supported by a bearing
N = Journal spinning speed (revolution per second)
P = Load per unit area of a bearing
R = Radius of journal
Re = Reynolds Number
Re_c = Critical Reynolds Number
U_x = Velocity of fluid in x direction
W = Static load supported by bearing
x = Cartesian coordinate
α_B = Real part of a complex Eigenvalue (backward mode)
α_F = Real part of a complex Eigenvalue (forward mode)
λ_B = Complex Eigenvalue (backward mode)
λ_F = Complex Eigenvalue (forward mode)
Ω_B = Imaginary part of a complex Eigenvalue (backward mode)
Ω_F = Imaginary part of a complex Eigenvalue (forward mode)
μ = Molten zinc viscosity
τ_{yx} = Shear stress induced in fluid
ω_{cr} = Spinning speed of journal at its threshold of instability
ρ = Molten zinc density

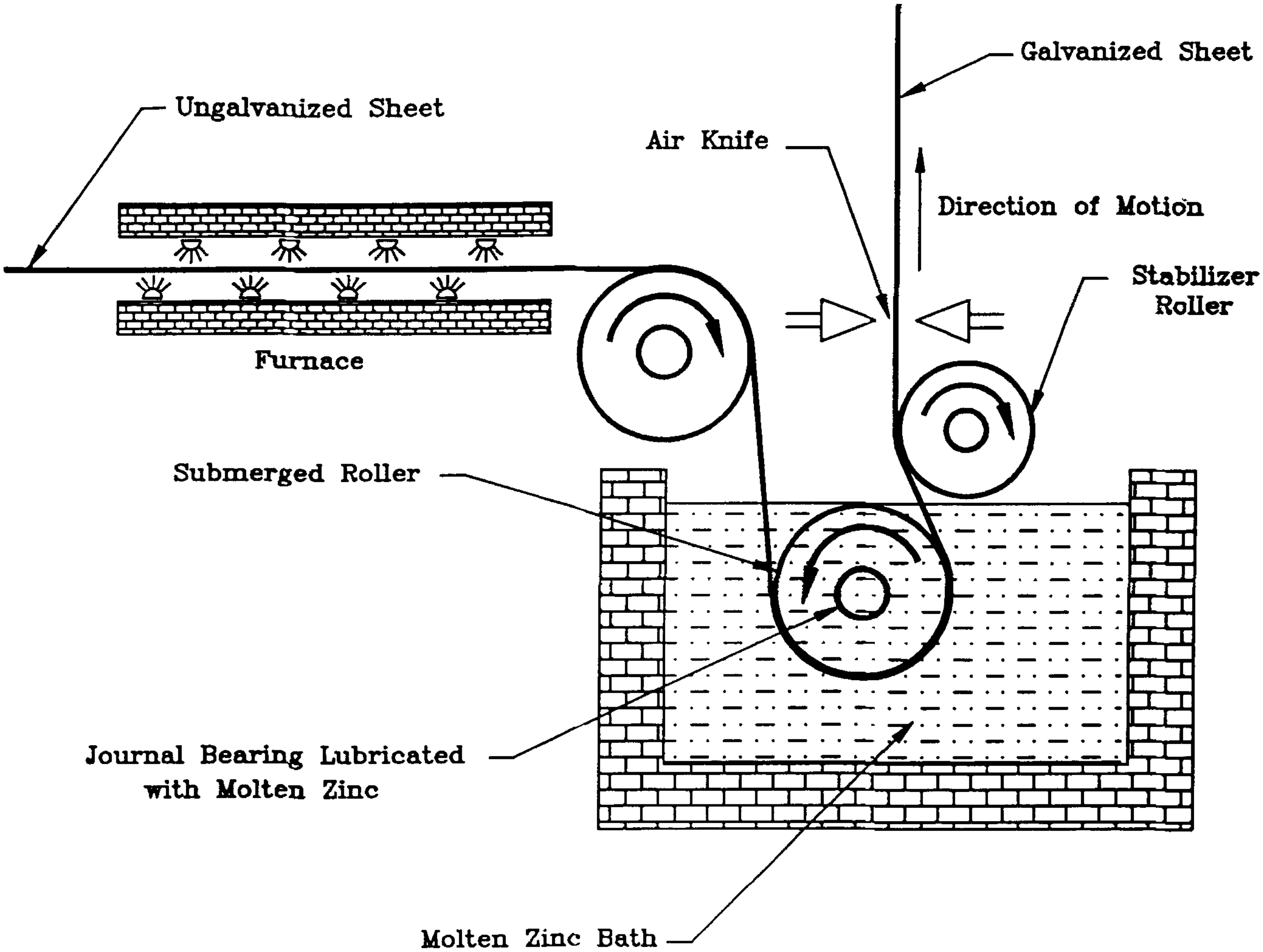

Fig. 1 Schematic view of galvanizing process.

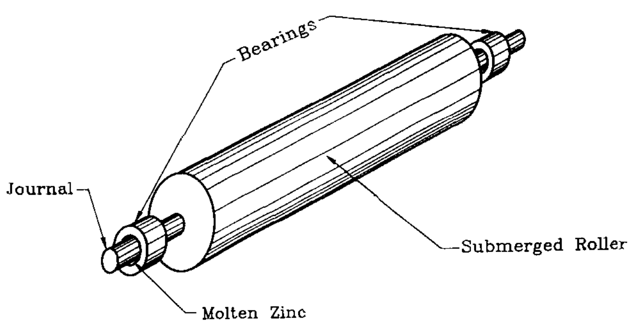

Fig. 2 Submerged roller supported by two journal bearings with molten zinc as lubricant.

controls the thickness of the zinc deposit on the metal sheet. Note that molten zinc is the lubricant of the journal bearings that support the rollers. The dynamic behavior of these bearings strongly influences the overall dynamics of the galvanizing process from a vibrational point of view. Bearing seizure, large roller lateral vibration amplitudes at certain production speeds, and frequent bearing failures are among the problems that have dictated a low rate of production in this process. Figure 2 shows a submerged roller in a molten zinc bath, with its two supporting journal bearings.

3. Journal Bearing and Molten Zinc as Lubricant

Theoretical and experimental investigations are numerous in the design/analysis of journal bearings.[1-7] In all previous work, the lubricant used in a journal bearing was either a compressible fluid (such as air), or incompressible fluid (such as a synthetic or natural oil, or water). The lubricant is either modeled as a Newtonian fluid or a non-Newtonian fluid.[4-7] See Ref 6 for a complete understanding of the differences between Newtonian and non-Newtonian fluids in hydrodynamic applications. Fluid viscosity and type of fluid (Newtonian or non-Newtonian) are the two major lubricant characteristics that influence the hydrodynamic properties of a journal bearing set. Knowledge of viscosity and type of fluid properties (Newtonian versus non-Newtonian) of zinc in its molten state therefore is the main factor in selecting the proper design/analysis of the

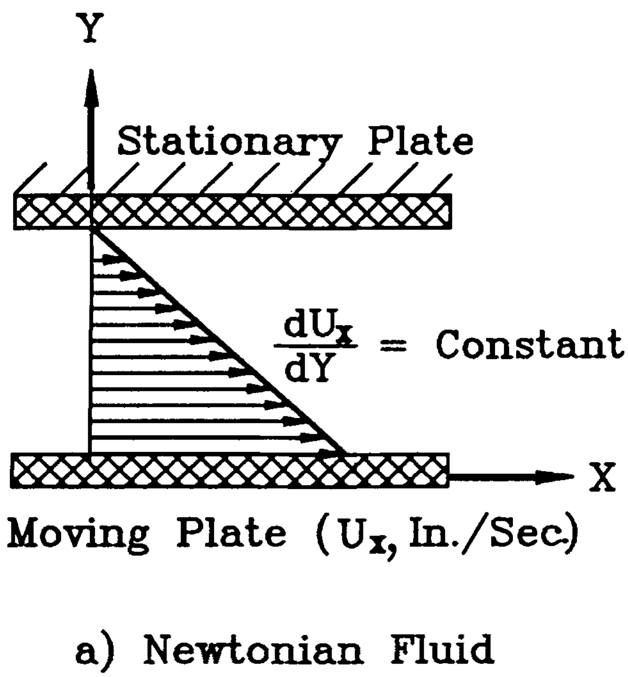

Fig. 3 Comparison of Newtonian and non-Newtonian fluids.

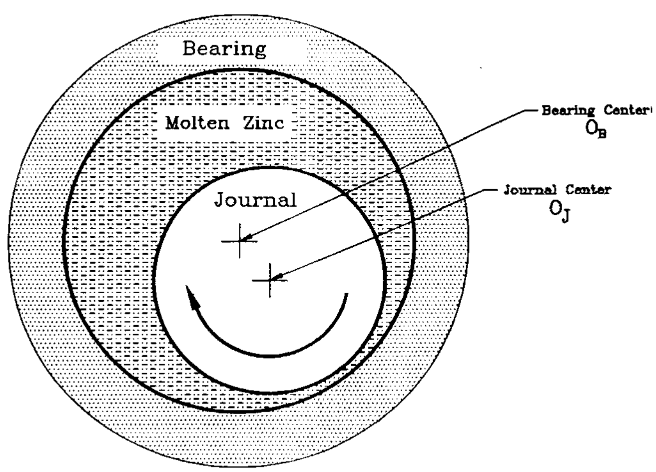

Fig. 4 Schematic view of a journal bearing with molten zinc lubricant.

journal bearings that support the guiding rollers in a galvanizing process.

4. Viscosity Characteristics of Molten Zinc

The viscosity of molten zinc has been determined both theoretically[8-11] and experimentally.[12] Previous work has shown that the viscosity of zinc in the molten state is strongly temperature dependent and composition dependent (*i.e.*, percentage of other elements such as Pb, Al, etc.), and is independent of pressure. Szekely[8] states that molten metals (including zinc) obey the Newtonian law of viscosity (see Fig. 3), *i.e.*,

$$\tau_{yx} = -\mu\,(dU_x/dY) \qquad [1]$$

Hence, to start formulating the design procedure for a journal bearing with molten zinc as the lubricant, one must begin with determining the viscosity of the zinc and zinc alloys in a molten state as a function of temperature. Yao and Kondic determined the viscosity of molten zinc experimentally.[12] Szekely[8] provides an analytical expression for determining the viscosity of molten metals (including zinc) in terms of the atomic properties of the metals (molecular weight, Boltzman's constant, etc.) and temperature. The results of the analytical approach is within 2% values of those obtained by Yao[12] and the values given in Ref 10.

5. Mathematical Modeling and Dynamic Analysis

In a galvanizing process, the molten zinc separates the rotating journal (roller) from the stationary bearing. Figure 4 shows a schematic view of a journal bearing set with molten zinc as the lubricant. The pressure developed in the radial clearance of the bearing supports the static load, as well as any dynamic load due to external disturbances or an imbalance of the roller. Here, the mechanical properties of the molten zinc are modeled by the standard stiffness and damper sets, as shown in Fig. 5. These stiffness and damper sets (hydrodynamic coefficients) determine the dynamic behavior of the rotating guide rollers. Assuming a symmetric roller, the system of the spinning and orbiting roller can be modeled as a two degrees of freedom inertia supported by the spring-damper elements mentioned earlier (see Fig. 5). The orbital motion of the journal (roller) in the cavity of the bearing is the purpose of the dynamic study and stability analysis in this work. The amplitude of the orbital motion of

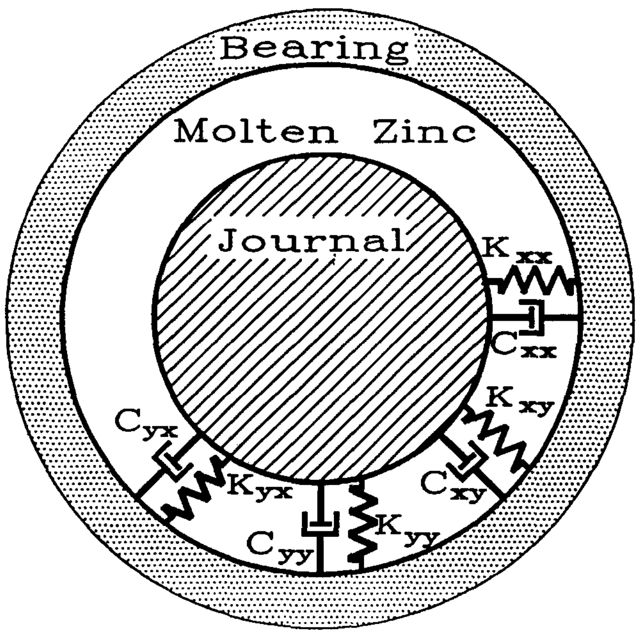

Fig. 5 Stiffness and damping properties of molten zinc (linearized model).

the roller is dictated by the bearing geometry, molten zinc properties, loads, and spinning speed of the roller. The standard dimensionless Sommerfeld number, S, expressed in Eq 2, summarizes the controlled or design parameters mentioned above. Knowledge of the Sommerfeld number enables one to determine the performance parameters of a journal bearing set such as the minimum lubricant film thickness, maximum pressure developed and its location, flow rate through the bearing, and the stability of the bearing.

$$S = (R/c)^2 \frac{\mu N}{P} \qquad [2]$$

Here, stability of the journal bearing means that the orbital motion of the roller is well within the limits of the geometric dimensions (radial clearance, c) of the bearing. The equation of orbital motion of the roller in the cavity of the bearing can be expressed as:

$$\begin{bmatrix} M & 0 \\ 0 & M \end{bmatrix} \begin{Bmatrix} \ddot{X} \\ \ddot{Y} \end{Bmatrix} + \begin{bmatrix} C_{xx} & C_{xy} \\ C_{yx} & C_{yy} \end{bmatrix} \begin{Bmatrix} \dot{X} \\ \dot{Y} \end{Bmatrix} + \begin{bmatrix} K_{xx} & K_{xy} \\ K_{yx} & K_{yy} \end{bmatrix} \begin{Bmatrix} X \\ Y \end{Bmatrix} = \begin{Bmatrix} f_x(t) \\ f_y(t) \end{Bmatrix} \qquad [3]$$

Unlike the ordinary inertia-stiffness-damping systems studied in classical vibration problems, the $[K]$ and $[C]$ matrices in Eq 3 are not symmetric. Hence, the possibility of a self-excited vibration exists for the orbital vibration of the roller. This self-excited vibration of the roller can grow in amplitude up to the threshold of instability at a given roller spinning speed, ω_{cr} (proportional to the galvanizing production speed). Any increase in the production speed will cause an instability of the orbital motion of the roller. The mechanism of this instability can be thought of as the impartation of energy from a spinning motion to that of the orbiting motion of the roller. Mathematically, this transfer of energy (instability mechanism) is related to the nonconservative force field stemming from the symmetric part of the $[C]$ matrix and the skew-symmetric part of the $[K]$ matrix. The Appendix contains the derivation of the energy impartation from/to the orbital motion.

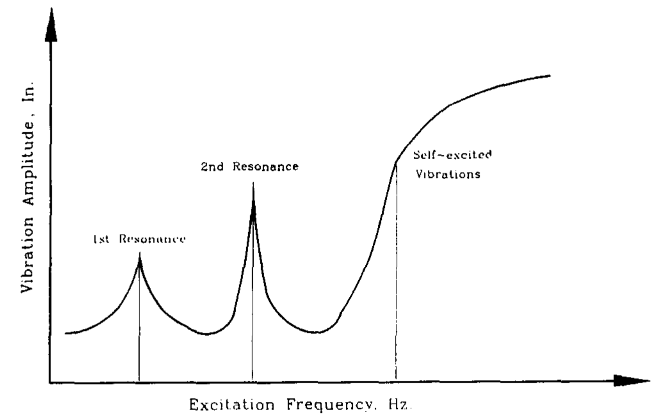

Fig. 6 Typical behavior of a vibratory system with resonance and self-excited instability characteristics.

The instability mechanism explained above is an undesirable condition in a galvanizing process. Here, one should note that this instability phenomenon is not a resonance condition; that is, the orbital motion amplitude does not decrease with increasing the spinning rate (galvanizing production rate). Figure 6 illustrates the typical behavior of the orbital motion of a spinning and orbiting journal versus the spinning speed of the journal. A properly designed journal bearing set for a galvanizing process, with molten zinc as its lubricant, must have its ω_{cr} such that the production speed can be maintained at an acceptably high rate.

6. Stability of the Galvanizing Roller

6.1 Eigenvalue Problem

The Eigenvalues of the linearized Eq 3 are complex numbers and can be determined by the standard method. These Eigenvalues have the following forms:

$$\begin{aligned} \lambda_B &= \alpha_B + \Omega_B j \\ \lambda_F &= \alpha_F + \Omega_F j \end{aligned} \qquad [4]$$

where $j = \sqrt{-1}$, and F and B denote the two modes (forward and backward) of the orbital vibration of the roller. The backward mode is always stable ($\alpha_B < 0$). Therefore, the real part of the forward mode Eigenvalue, α_F, determines the stability of the journal bearing lubricated with molten zinc. If $\alpha_F > 0$, then E_{cyc} derived in the Appendix will be positive, which means that the orbital motion of the roller will grow in amplitude (instability). If $\alpha_F = 0$, the bearing will be at its threshold of instability; $\alpha_F < 0$ means the system is stable.

Table 1 Controlled Parameters of Journal Bearing with Molten Zinc Lubricant

Bearing load (W), N	lb	Bearing diameter (D), m	in.	Radial clearance (C), m	in.	Roller speed (N), rpm
3115	700	0.25	10	5.1×10^{-5}	0.002	424

Table 2 Viscosity of Molten Zinc Alloys at Various Temperatures

Temperature, °C	°F	100% zinc MPa·sec × 10^9	100% zinc Re × 10^7	97.5% zinc MPa·sec × 10^9	97.5% zinc Re × 10^7	95% zinc MPa·sec × 10^9	95% zinc Re × 10^7	86% zinc MPa·sec × 10^9	86% zinc Re × 10^7
232.8	450	2.85	4.14	2.40	3.48	2.20	3.19	1.76	2.55
287.8	550	2.38	3.45	2.05	2.98	1.85	2.69	1.50	2.18
343.3	650	2.08	3.02	1.68	2.44	1.60	2.32	1.30	1.89
398.9	750	1.83	2.66	1.58	2.29	1.42	2.06	1.15	1.67
454.4	850	1.65	2.39	1.30	1.89	1.28	1.86	1.07	1.55

Table 3 Sommerfeld Number of the Lubrication Regime with Molten Zinc Lubricant ($L/D = 1$)

Temperature, °C	°F	Sommerfeld No. of: 100% zinc	97.5% zinc	95% zinc	86% zinc
232.8	450	0.64	0.54	0.50	0.40
287.8	550	0.54	0.46	0.42	0.34
343.3	650	0.48	0.38	0.36	0.30
398.9	750	0.42	0.36	0.32	0.26
454.4	850	0.38	0.30	0.30	0.24

Table 4 Sommerfeld Number of the Lubrication Regime with Molten Zinc Lubricant ($L/D = 0.5$)

Temperature, °C	°F	Sommerfeld No. of: 100% zinc	97.5% zinc	95% zinc	86% zinc
232.8	450	0.32	0.27	0.25	0.20
287.8	550	0.27	0.23	0.21	0.17
343.3	650	0.24	0.19	0.18	0.15
398.9	750	0.21	0.18	0.16	0.13
454.4	850	0.19	0.15	0.15	0.12

7. Example

Using the viscosity values obtained from Ref 11, a set of computer-simulated test cases are presented here. Table 1 contains selected values of the design (controlled) parameters for a journal bearing lubricated with molten zinc for a typical roller geometry, bearing load, and journal speed shown in Fig. 2. The journal rotational speed given in Table 1 (424 rpm) is equivalent to the galvanizing production rate of 2.54 m/sec (500 ft/min). Table 2 includes the viscosities of different molten zinc alloys at various temperatures. The Sommerfeld numbers of the lubrication regimes associated with each zinc alloy composition and operating temperature are given in Tables 3 and 4 for L/D ratios of 1.0 and 0.5, respectively. The stiffness and damping properties of the lubrication regimes are given in Tables 5 and 6. The damping and stiffness parameters given in Tables 5 and 6 are in the following dimensionless forms:[2]

$$K_{mn} = \frac{c\overline{K}_{mn}}{W} \text{ and } C_{mn} = \frac{c\omega\overline{C}_{mn}}{W} \quad \text{m and n = x and y} \qquad [5]$$

where $\overline{K}_{mn}$ and $\overline{C}_{mn}$ are the dimensional stiffness and damping properties of the bearing. The dimensionless mass associated with the dimensionless parameters given by Eq 5 is:

$$M = \frac{c\,\omega^2\,\overline{M}}{W} \qquad [6]$$

where $\overline{M}$ is the dimensional mass supported by each bearing. The results of the stability analysis mentioned earlier are summarized in Table 7, which gives the minimum molten zinc film thickness as well as the Eigenvalues of the two degrees of freedom system presented earlier. Table 5 shows that all the Eigenvalues have negative real parts, which indicates stable operating conditions as discussed above.

8. Turbulent Versus Laminar Fluid Film Flow Consideration

Generally, transition from laminar to turbulent flow occurs when the Reynolds number of the flow exceeds a critical value.

Table 5 Dimensionless Stiffness and Damping Properties of Molten Zinc Alloys Acting as the Bearing Lubricant in a Galvanizing Process ($L/D = 1$)

S	K_{xx}	K_{xy}	K_{yx}	K_{yy}	C_{xx}	C_{xy}	C_{yx}	C_{yy}
0.24	1.70	3.40	−1.65	2.10	5.25	2.10	2.35	4.75
0.26	1.60	3.50	−1.80	2.11	6.43	2.18	2.35	5.01
0.30	1.50	3.65	−2.20	2.11	6.79	2.20	2.30	5.54
0.32	1.45	3.80	−2.40	2.12	6.98	2.18	2.27	5.80
0.34	1.44	3.90	−2.50	2.13	7.18	2.17	2.25	6.06
0.36	1.43	4.00	−2.70	2.13	7.37	2.16	2.23	6.33
0.38	1.42	4.20	−2.90	2.14	7.57	2.13	2.21	6.59
0.40	1.40	4.25	−3.00	2.14	7.78	2.10	2.20	6.85
0.42	1.38	4.50	−3.20	2.15	7.98	2.50	2.20	7.11
0.46	1.35	4.75	−3.50	2.16	8.41	2.20	2.20	7.64
0.48	1.34	4.85	−3.60	2.16	8.63	2.08	2.20	7.90
0.50	1.33	5.00	−3.80	2.17	8.85	2.00	2.20	8.17
0.54	1.30	5.40	−4.20	2.18	9.30	2.00	2.20	8.69
0.64	1.20	6.20	−5.00	2.20	10.50	2.00	2.20	10.00

Table 6 Dimensionless Stiffness and Damping Properties of Molten Zinc Alloys Acting as the Bearing Lubricant in a Galvanizing Process ($L/D = 0.5$)

S	K_{xx}	K_{xy}	K_{yx}	K_{yy}	C_{xx}	C_{xy}	C_{yx}	C_{yy}
0.12	6.50	4.50	0.20	1.70	7.50	2.50	2.50	1.50
0.13	6.35	4.44	0.18	1.73	7.44	2.52	2.52	1.54
0.15	6.04	4.31	0.13	1.78	7.31	2.55	2.55	1.62
0.16	5.88	4.25	0.11	1.80	7.25	2.56	2.56	1.66
0.18	5.57	4.13	0.08	1.85	7.13	2.59	2.59	1.74
0.19	5.42	4.06	0.06	1.88	7.06	2.61	2.61	1.78
0.20	5.26	4.00	0.05	1.90	7.00	2.62	2.62	1.82
0.21	5.11	3.98	0.02	1.92	6.96	2.64	2.64	1.86
0.23	4.80	3.94	−0.02	1.95	6.87	2.68	2.68	1.94
0.24	4.64	3.92	−0.04	1.97	6.83	2.68	2.68	1.98
0.25	4.49	3.90	−0.06	1.98	6.79	2.70	2.70	2.02
0.27	4.18	3.86	−0.10	2.02	6.71	2.73	2.73	2.10
0.32	3.40	3.75	−0.22	2.10	6.50	2.80	2.80	2.30

This flow regime transition is of particular interest in hydrodynamic bearings, because the fluid film properties (load-carrying capacity, friction, etc.) are modified as the bearing flow regime changes from laminar to turbulent. The value of critical Reynolds number varies for different types of fluid flows. The following is a summary of critical Reynolds numbers, Re_c, associated with various flow types:

Flow in pipes and tubes: $Re_c = 2000$ [7]

Hydrodynamic journal bearing with no externally pressurized lubricant feed:[13] $Re_c = 41.1/\sqrt{(2c/D)}$ [8]

Hydrodynamic thrust bearing:[14] $Re_c = 1000$ [9]

Hydrodynamic journal bearings externally pressurized:[15] $Re_c = 500$ [10]

The journal bearing presented in this article has a critical Reynolds number described by Eq 8, and is calculated as:

$$Re_c = 41.1/\sqrt{(2 \cdot 5.1 \times 10^{-5}/0.25)} = 2034.8 \quad [11]$$

The Reynolds number of a journal bearing under a given operating condition is determined from:

$$Re = \pi\, D\, N\, c\, \rho/\mu \quad [12]$$

where D is the bearing diameter, m; N is the bearing speed, rps; c is the radial clearance, m; μ is the fluid viscosity, Pa-sec.; and ρ is the lubricant density, kg/m^3.

Table 8 shows the density of pure molten zinc at different temperatures.[16] Using the data given in this table along with the molten zinc (pure) viscosity, bearing geometry, and the bearing speed, the Reynolds number of each operating temperature may be calculated via Eq 12. The results are shown in Table 9.

Comparing the results of Table 9 with the critical Reynolds numbers given in Eq 11 indicates that the bearing system considered in this work maintains a laminar flow regime within the molten zinc film thickness at the different assumed operating temperatures.

9. Conclusions

The behavior of a journal bearing lubricated with molten zinc is studied in this work. The sheet metal galvanizing process uses bearings of such to support guiding rollers. The stability of bearings with a molten zinc lubricant were examined. The bearing geometry and the temperature of the molten zinc bath

Table 7 Results of Stability Analysis (Eigenvalues)

S	Minimum film thickness $m \times 10^5$	Minimum film thickness in. $\times 10^3$	Eigenvalues $\times 10^{-3}$
$L/D = 1$			
0.24	2.84	1.12	−1.6686 −0.6307 $-0.0003 \pm 0.0005j$
0.26	3.00	1.18	−1.6181 −0.6693 $-0.0003 \pm 0.0005j$
0.30	3.15	1.24	−0.6996 −0.7658 $-0.0003 \pm 0.0005j$
0.32	3.25	1.28	−1.7796 −0.8678 $-0.0003 \pm 0.0005j$
0.34	3.30	1.30	−1.7797 −0.8678 $-0.0003 \pm 0.0005j$
0.36	3.35	1.32	−1.8208 −0.9186 $-0.0003 \pm 0.0005j$
0.38	3.45	1.36	−1.8608 −0.9709 $-0.0002 \pm 0.0005j$
0.40	3.51	1.38	−1.9026 −1.0229 $-0.0002 \pm 0.0005j$
0.42	3.56	1.40	−1.9858 −1.0317 $-0.0002 \pm 0.0005j$
0.46	3.61	1.42	−2.0516 −1.1581 $-0.0002 \pm 0.0005j$
0.48	3.66	1.44	−2.0888 −1.2188 $-0.0002 \pm 0.0005j$
0.50	3.71	1.46	−2.1268 −1.2768 $-0.0002 \pm 0.0005j$
0.54	3.86	1.52	−2.2227 −1.3749 $-0.0002 \pm 0.0005j$
0.64	4.01	1.58	−2.4723 −1.6274 $-0.0002 \pm 0.0006j$
$L/D = 0.5$			
0.12	1.22	0.48	−1.6801 −0.1187 $-0.0006 \pm 0.0001j$
0.13	1.27	0.50	−1.6731 −0.1207 $-0.0011 \pm 0.0009j$
0.15	1.37	0.54	−1.6583 −0.1276 $-0.0011 \pm 0.0009j$
0.16	1.42	0.56	−0.6482 −0.1317 $-0.0011 \pm 0.0009j$
0.18	1.52	0.60	−0.6338 −0.1381 $-0.0011 \pm 0.0008j$
0.19	1.57	0.62	−1.6257 −0.1402 $-0.0011 \pm 0.0008j$
0.20	1.63	0.64	−1.6181 −0.1439 $-0.0010 \pm 0.0008j$
0.21	1.68	0.66	−2.1483 −0.2141 $-0.0008 \pm 0.0005j$
0.23	1.78	0.70	−1.6086 −0.1514 $-0.0010 \pm 0.0008j$
0.24	1.83	0.72	−1.6032 −0.1569 $-0.0010 \pm 0.0007j$
0.25	1.88	0.74	−1.6008 −0.1593 $-0.0009 \pm 0.0007j$
0.27	1.93	0.76	−1.5949 −0.1652 $-0.0009 \pm 0.0007j$
0.32	2.03	0.80	−1.5794 −0.1789 $-0.0008 \pm 0.0007j$

Table 8 Density of Pure Molten Zinc at Different Temperatures

Temperature, °C	Density, kg/m^3
450	6.60×10^3
550	6.50×10^3
650	6.40×10^3
750	6.30×10^3
850	6.20×10^3

Table 9 Reynolds Number of Journal Bearing Lubricated with Pure Molten Zinc at Different Operating Temperatures

Temperature, °C	Reynolds No.
450	655.5
550	773.1
650	870.9
750	974.5
850	1063.1

can be adjusted so that for a given zinc alloy composition the production speed (rollers speed) does not fall in the instability region of the bearing. The molten zinc is modeled as a Newtonian fluid in this work (supported by Ref 8). Further improvements of the bearing dynamic analysis can be achieved by including the inertia effects of the molten zinc in the hydrodynamic equations of bearing performance (Eq 3). Inclusion of the molten zinc inertia effects will be undertaken by the author in a subsequent article. A major assumption made in this work is that no chemical reactions take place between the molten zinc and journal bearing material(s). Any chemical reaction may affect the mechanical properties of the molten zinc within the bearing radial clearance; this would influence the bearing performance.

References

1. P.G. Morton, Dynamic Characteristics of Bearings Measurements Under Operating Condition, *GEC J. Sci. Technol.*, *42*, 37-47 (1975).
2. J.W. Lund, E.B. Arwas, H.S. Chen, C.W. Ng, C.H.T. Pan, and B. Sternlich, "Rotor Bearing Dynamics Technology, Part 3," Wright-Patterson Air Force Base, OH, Technical Report AFAPL TR-65-45 (1965).
3. D.W. Parkins, Theoretical and Experimental Determination of the Dynamic Characteristics of Hydrodynamic Journal Bearings, *J. Lub. Technol.*, *101*, 129-139, Apr (1979).
4. P.D. Williams and G.R. Symmons, Analysis of Hydrodynamic Slider Thrust Bearings Lubricated With Non-Newtonian Fluids, *Wear*, *117*, 91-102 (1987).
5. B. Najji, B. Bou-Said, and D. Berthe, New Formulation for Lubrication With Non-Newtonian Fluids, *ASME Trans., J. Tribol.*, *111*, 29-34, Jan (1989).
6. J.F. Hutton, K.P. Jackson, and B.P. Williamson, The Effects of Lubricant Rheology on the Performance of Journal Bearings, *ASLE Trans.*, *29*(1), 52-60 (1984).
7. R.H. Buckholz, On the Role of a Non-Newtonian Fluid in Short Bearing Theory, *ASME Trans., J. Tribol.*, *107*, 69-74, Jan (1985).
8. J. Szekely, *Fluid Flow Phenomena in Metals Processing*, Academic Press, New York (1979).
9. G.H. Geiger and D.R. Poirier, *Transport Phenomena in Metallurgy*, Addison-Wesley, Boston (1973).
10. S. Mitsuo, *Liquid Metals, An Introduction to the Physics and Chemistry of Metals in the Liquid State*, Academic Press, New York (1977).
11. S.Z. Beer, *Liquid Metals, Chemistry and Physics*, Marcel Dekker, New York (1972).
12. T.P. Yao and V. Kondic, The Viscosity of Molten Tin, Lead, Zinc, Aluminum, and Some of Their Alloys, *J. Inst. Metals*, *81*, 17-24 (1952-1953).
13. G.I. Taylor, Stability of a Viscous Liquid Contained Between Two Rotating Cylinders, *Phil. Trans., Roy. Soc., London, Ser. A*, *223*, 289-343 (1923).
14. S. Abramowitz, Turbulence in a Tilting Pad Thrust Bearing, *Trans. ASME*, *78*, 1-6 (1956).
15. D.F. Wilcock, Turbulence in High-Speed Journal Bearings, *Trans. ASME*, *72*, 825-834 (1950).
16. *Metals Handbook*, American Society for Metals, Metals Park, 1078-1088 (1948).

Appendix

Derivation of the energy imparted to a journal, E_{cyc}, in terms of the symmetric part of the lubricant damping and the skew-symmetric part of the lubricant stiffness matrices:

Assume sinusoidal X and Y components of the orbital motion of the journal, as expressed by Eq 1 (see Fig. 1):

$$\{\vec{X}\} = \begin{Bmatrix} X\sin(\Omega t+\theta_x) \\ Y\sin(\Omega t+\theta_y) \end{Bmatrix} \quad [1]$$

The skew-symmetric part of the stiffness and the symmetric part of the damping matrices constitute the nonconservative force field in this model. The nonconservative force due to the damping and stiffness matrices are given in Eq 2 and Eq 3, respectively:

$$C^s\vec{X} = \begin{Bmatrix} \Omega X C^s_{xx}\cos(\Omega t+\theta_x) + \Omega Y C^s_{xy}\cos(\Omega t+\theta_y) \\ \Omega X C^s_{xy}\cos(\Omega t+\theta_x) + \Omega Y C^s_{yy}\cos(\Omega t+\theta_y) \end{Bmatrix} \quad [2]$$

$$K^{ss}\vec{X} = \begin{Bmatrix} K^{ss}_{xy} Y\sin(\Omega t+\theta_y) \\ -K^{ss}_{xy} X\sin(\Omega t+\theta_x) \end{Bmatrix} \quad [3]$$

The total nonconservative force vector, $\vec{P}$, becomes:

$$\vec{P} = -(C^s\vec{X} + K^{ss}\vec{X}) \quad [4]$$

Substituting Eq 2 and Eq 3 into Eq 4 yields:

$$\vec{P} = -\begin{Bmatrix} \Omega C^s_{xx} X\cos(\Omega t+\theta_x) + \Omega C^s_{xy} Y\cos(\Omega t+\theta_y) + X^{ss}_{xy} Y\sin(\Omega t+\theta_y) \\ \Omega C^s_{xy} X\cos(\Omega t+\theta_x) + \Omega C^s_{yy} Y\cos(\Omega t+\theta_y) - K^{ss}_{xy} X\sin(\Omega t+\theta_x) \end{Bmatrix} \quad [5]$$

The imparted energy per cycle is defined as E_{cyc}, which is the integral of the nonconservative force vector over one orbital cycle:

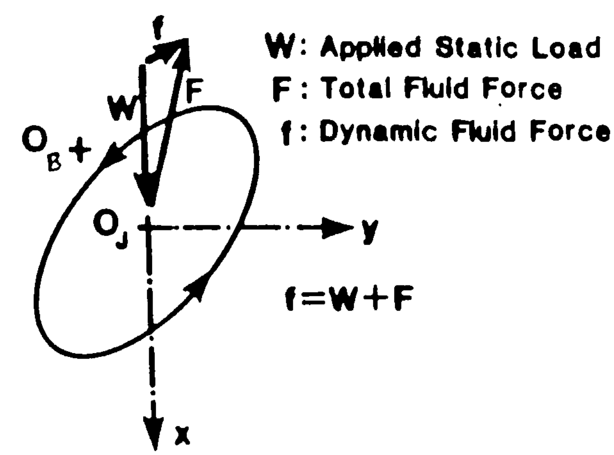

Fig. 1 Sinusoidal orbital motion of journal relative to bearing; X and Y are referenced to static equilibrium state (only spinning motion), $X = x\sin(\Omega t + \Theta_x)$, $Y - y\sin(\Omega t + \Theta_y)$

$$E_{cyc} = \oint \vec{P} \cdot d\vec{X} \quad [6]$$

where dX is:

$$\{\vec{dX}\} = \begin{Bmatrix} \Omega\, X \cos(\Omega t + \theta_x) \\ \Omega\, Y \cos(\Omega t + \theta_y) \end{Bmatrix} \quad [7]$$

The result of $\vec{P} \cdot \vec{dX}$ can be summarized as:

$$\begin{aligned} \vec{P} \cdot \vec{dX} = -\Big[& \Omega^2 C^s_{xx} X^2 \cos^2(\Omega t + \theta_x) \\ & + \Omega^2 C^s_{xy} X\, Y \cos(\Omega t + \theta_x) \cdot \cos(\Omega t + \theta_y) \\ & + \Omega^2 K^{ss}_{xy} X\, Y \cos(\Omega t + \theta_x) \cdot \sin(\Omega t + \theta_y) \\ & + \Omega^2 Y^2 \cos^2(\Omega t + \theta_y) + \Omega^2 C^s_{xy} X\, Y \cos(\Omega t + \theta_y) \\ & \cdot \cos(\Omega t + \theta_x) - \Omega^2 K^{ss}_{xy} X\, Y \cos(\Omega t + \theta_y) \\ & \cdot \sin(\Omega t + \theta_x) \Big] dt \end{aligned} \quad [8]$$

Substituting Eq 8 into Eq 6 and taking the integral over one cycle of the orbital motion of the journal yields:

$$\begin{aligned} E_{cyc} = -\Big[& C^s_{xx} X^2 \Omega^2 \int_0^{2\pi/\Omega} \cos(\Omega t + \theta_x)\, dt \\ & + 2C^s_{xy} X\, Y\, \Omega^2 \int_0^{2\pi/\Omega} \cos(\Omega t + \theta_x) \cdot \cos(\Omega t + \theta_y)\, dt \\ & - K^{ss}_{xy} X\, Y\, \Omega^2 \int_0^{2\pi/\Omega} \sin\left(\theta_x - \theta_y\right) dt \\ & + C^s_{xy} Y^2 \Omega^2 \int_0^{2\pi/\Omega} \cos(\Omega t + \theta_y)\, dt \Big] \end{aligned} \quad [9]$$

Taking the integrals expressed in Eq 9, the final form of E_{cyc} becomes:

$$\begin{aligned} E_{cyc} = -\Big[& \Omega \left(C^s_{xx} X^2 + 2C^s_{xy} X\, Y \cos\left(\theta_x - \theta_y\right) + C^s_{yy} Y^2 \right) \\ & - 2K^{ss}_{xy} X\, Y \sin\left(\theta_x - \theta_y\right) \Big] \end{aligned} \quad [10]$$